

# Electron impact excitation cross sections for hydrogen-like ions

Vladimir Fisher, Yuri V. Ralchenko, Vladimir Bernshtam, Alexander Goldgirsh, and Yitzhak Maron  
*Faculty of Physics, Weizmann Institute of Science,  
Rehovot 76100, Israel*

Leonid A. Vainshtein  
*P. N. Lebedev Physical Institute, Russian Academy of Sciences,  
Moscow 117924, Russia*

Igor Bray  
*Electronic Structure of Materials Centre, School of Physical Sciences,  
The Flinders University of South Australia, G.P.O. Box 2100,  
Adelaide 5001, Australia*

Helen Golten  
*Churchill College, Cambridge, United Kingdom*  
(Received 20 June, 1996)

We present cross sections for electron-impact-induced transitions  $n \rightarrow n'$  in hydrogen-like ions  $C^{5+}$ ,  $Ne^{9+}$ ,  $Al^{12+}$ , and  $Ar^{17+}$ . The cross sections are computed by Coulomb-Born with exchange and normalization (CBE) method for all transitions with  $n < n' < 7$  and by convergent close-coupling (CCC) method for transitions with  $n < n' < 5$  in  $C^{5+}$  and  $Al^{12+}$ . Cross sections  $1s \rightarrow 2s$  and  $1s \rightarrow 2p$  are presented as well. The CCC and CBE cross sections agree to better than 10% with each other and with earlier close-coupling results (available for transition  $1 \rightarrow 2$  only). Analytical expression for  $n \rightarrow n'$  cross sections and semiempirical formulae are discussed.

PACS number(s): 34.80.Kw

## I. INTRODUCTION

Progress in many plasma physics fields (such as kinetics of incompletely ionized plasmas, radiative hydrodynamics of non-equilibrium plasmas, interpretation of spectroscopic measurements, etc.) depends on availability and accuracy of electron-ion inelastic collision cross sections. In this paper we present high-accuracy cross sections for electron-impact-induced transitions between  $n$ -states of some hydrogen-like ions, namely, for transitions  $n \rightarrow n'$  with  $n < n' < 7$  in ions  $C^{5+}$ ,  $Ne^{9+}$ ,  $Al^{12+}$ , and  $Ar^{17+}$ . The cross sections are denoted by  $\sigma_{z,n,n'}(x)$  where  $z$  is the ion nuclear charge,  $n$  and  $n'$  are the principal quantum numbers of initial and final states respectively ( $n' > n$ ), and

$$x = \varepsilon/E_{nn'}$$

is the ratio of the incident electron kinetic energy  $\varepsilon$  to transition energy  $E_{n,n'}$ . The cross sections are computed by the Coulomb-Born with exchange and normalization (CBE) method [1,2] and by the convergent close-coupling (CCC) method [3-5].

In Sec. II, we present and compare the CCC and CBE cross sections together with earlier close-coupling (CC) results [6-8]. However, the CC cross sections are published for transition  $1 \rightarrow 2$  only. We do not include comparisons with broad-energy-range cross sections calculated by less accurate methods (for assessment of theoretical data sources see papers by Pradhan and Gallagher [9] and Callaway [10]). For use in applications, Sec. III contains a table of coefficients which provide good analytical fit to all  $n \rightarrow n'$  cross sections discussed in Sec. II. Two semiempirical formulae for the cross section estimates are discussed in Sections IV and V.

## II. THE CROSS SECTIONS

The CBE cross sections were calculated by computer code ATOM [1]. In this code, the exchange is accounted by method of orthogonalized functions and the normalization is done by K-matrix method using one own channel [2]. Being installed on a personal computer, code ATOM provides dozens of cross sections per day.

The CCC method is presented in Refs. [3,4]. The basic idea of the CCC approach to electron-atom and electron-ion collisions is to solve the coupled equations arising upon expansion of the total wave function in a truncated Laguerre basis of size  $N$ . This basis size is increased until convergence to a desired accuracy is observed. The usage of the

Laguerre basis ensures that all states in the expansion are square-integrable, and so gives a discretization of the target continuum as well as a good representation of the target true discrete spectrum. For a sufficiently large  $N$  pseudoresonances, associated with the target continuum discretization, diminish substantially so that no averaging is necessary. The presented CCC calculations at all given energies are likely to be within 10% of the true non-relativistic model solution for the considered scattering systems. In general, the CCC method demonstrates excellent agreement with experimental results available for various targets [3–5].

The CCC and CBE computer codes produce cross sections for  $nl \rightarrow n'l'$  transitions. These cross sections are denoted below by  $\sigma_{z,nl,n'l'}(x)$ . To obtain the cross sections for the  $n \rightarrow n'$  transitions, partial cross sections  $\sigma_{z,nl,n'l'}(x)$  are summed over  $l'$  and averaged over  $l$ :

$$\sigma_{z,n,n'}(x) = \sum_{l=0}^{n-1} g_{nl} g_n^{-1} \sum_{l'=0}^{n'-1} \sigma_{z,nl,n'l'}(x) \quad (1)$$

Here  $g_{nl}$  and  $g_n = \sum_l g_{nl}$  are statistical weights of states  $nl$  and  $n$  respectively. Statistical averaging over  $l$  (which is reflected by the factor  $g_{nl} g_n^{-1}$ ) is caused by uncertainty of  $l$  in initial quantum state given by  $n$  only. Summation over  $l'$  ensures inclusion of all possible final states for a given  $n'$  of interest.

The cross sections  $\sigma_{z,n,n'}(x)$  are presented in Figs. 1–8. One can see: (i) the CBE cross sections for all transitions with  $n < n' < 7$  in ions  $C^{5+}$ ,  $Ne^{9+}$ ,  $Al^{12+}$ , and  $Ar^{17+}$ ; (ii) the CCC cross sections for all transitions with  $n < n' < 5$  in ions  $C^{5+}$  and  $Al^{12+}$ ; and (iii) the CC results available for transition  $1 \rightarrow 2$  in ions  $C^{5+}$ ,  $O^{7+}$ ,  $Ar^{17+}$  and  $Fe^{25+}$  [6–8]. To emphasize the scaling of the cross sections over  $z^4$ , we present scaled cross sections  $z^4 \sigma_{z,n,n'}(x)$ . For  $x \gg 1$  these are independent of  $z$  to an accuracy better than 1%. For  $x \sim 1$  there is a weak dependence on  $z$  which results in small deviations from the scaling. These deviations are to within 5% for  $z = 10 \div 18$  and to within 10% for  $z = 6$  (except for transition  $5 \rightarrow 6$  in  $C^{5+}$  which deviates by 17% at  $x \rightarrow 1$ ). In present paper we limit our consideration by  $z > 5$  but it should be mentioned that for  $z \leq 5$  deviations from the  $z^4$ -scaling are more significant, for example: 40% for transition  $1 \rightarrow 2$  in  $He^+$  and a factor of 3 for transition  $5 \rightarrow 6$  in  $He^+$ .

To see the difference between CCC, CC, and CBE results with no influence of  $z^4$ -scaling, one may compare the cross sections related to the same ion. However, the data available enables to compare the three approximations for a single transition only, namely, for transition  $1 \rightarrow 2$  in  $C^{5+}$  (Fig. 1). For this transition the CCC, CC, and CBE cross sections deviate from each other by less than 8%. Generally, the CCC and CBE cross sections of any transition studied deviate from each other by less than 10%. Note, that in present work we do not compare broad-energy-range cross sections to cross sections computed exclusively for narrow energy intervals where contributions of resonances are significant (see, e.g., Refs. [9,12,13]). Such fine detail is not necessary for the purpose of most applications.

Figs. 9 and 10 demonstrate excellent agreement between the CCC, CC, and CBE results for both monopole ( $l' = l$ ) and dipole ( $l' = l \pm 1$ ) channels contributing to transition  $1 \rightarrow 2$ . At  $x \approx 1$ , cross section  $1s \rightarrow 2p$  is larger than  $1s \rightarrow 2s$  by a factor of 4; with  $x$  the cross section  $1s \rightarrow 2p$  goes down slower than  $1s \rightarrow 2s$  (namely, as  $x^{-1} \ln x$  vs.  $x^{-1}$ ), therefore the  $1 \rightarrow 2$  cross section is almost exclusively due to the dipole channel. In general, in double sums (1) contributions from dipole transitions dominate over contributions from non-dipole ones. Therefore, properties of non-dipole cross sections are practically indistinguishable in total cross sections  $\sigma_{z,n,n'}(x)$ . Properties of partial cross sections  $\sigma_{z,nl,n'l'}(x)$  will be discussed in separate paper [14] which, in particular, demonstrates (i) strong effect of electron exchange for energy range  $x < 3$ , and (ii) an increase of this effect with multipole order  $|l' - l|$ .

### III. FITTING FORMULA

To simplify a use of the cross sections in applications, we fitted them by analytical function. Taking account for the  $z^4$ -scaling and analysis presented in Ref. [15] the fitting function is chosen to be

$$\sigma_{z,n,n'}^f(x) = \pi a_0^2 z^{-4} x^{-1} (\alpha_{n,n'} \ln x + \beta_{n,n'} x^{-1} \ln x + \gamma_{n,n'} + \delta_{n,n'} x^{-1} + \zeta_{n,n'} x^{-2}) . \quad (2)$$

Here  $a_0$  is the Bohr radius. Coefficients  $\alpha_{n,n'}$ ,  $\beta_{n,n'}$ ,  $\gamma_{n,n'}$ ,  $\delta_{n,n'}$ , and  $\zeta_{n,n'}$  are listed in Table 1. The fitting function  $\sigma_{z,n,n'}^f(x)$  provides an accuracy to better than 10% for any  $x$  for all transitions studied ( $z = 6 \div 26$ ) except for transition  $5 \rightarrow 6$  in  $C^{5+}$ . For this transition, the fit is less accurate because at  $x \rightarrow 1$  the cross section deviates by 17% from total scaling over  $z^4$  (Fig. 8).

#### IV. THE VAN REGEMORTER FORMULA

Expression (2) may be used in applications which require high accuracy of the cross sections. For estimates, it is desirable to have a simpler expression which does not use a table of coefficients. Frequently, such estimates are based on the Van Regemorter formula [2,9,11,16–20]. For transitions between  $n$ -states this formula may be presented as follows

$$\sigma_{z,n,n'}^{VR}(x) = \pi a_0^2 \frac{8\pi f_{nn'}}{\sqrt{3}} \frac{\mathcal{R}^2}{E_{nn'}^2} \frac{G(x)}{x}. \quad (3)$$

Here  $f_{nn'}$  is the absorption oscillator strength,  $\mathcal{R} = 13.6$  eV is the Rydberg energy unit, and  $G(x)$  is the effective Gaunt factor which may be treated as a fitting function of order unity.

To find an accurate expression for the  $n$ -independent function  $G(x)$ , we first use fitting function (2) and Eq. (3) to introduce the Gaunt factor  $G_{nn'}(x)$  for each of transitions studied:

$$G_{nn'}(x) = x \sigma_{z,n,n'}^f(x) \left( \pi a_0^2 \frac{8\pi f_{nn'}}{\sqrt{3}} \frac{\mathcal{R}^2}{E_{nn'}^2} \right)^{-1}.$$

These Gaunt factors for all transitions with  $n < n' < 7$  are shown by dotted curves in Fig. 11. The curves are not labeled because they are shown only for demonstrating the small spread of functions  $G_{nn'}(x)$  near their mean function

$$G(x) = 0.349 \ln x + 0.0988 + 0.455x^{-1} \quad (4)$$

which is shown by bold solid curve. We recommend function (4) as effective Gaunt factor for the Van Regemorter formula (3).

Bold dot-dash curves in Fig. 11 show  $\pm 50\%$  corridor around this  $G(x)$ . One can see that for  $x \approx 1$  some dotted curves deviate from  $G(x)$  by more than a factor of 2, but for  $x > 5$  a spread of dotted curves is smaller (to within  $\pm 50\%$ ), and for  $x = 100 \div 1000$  the spread is to within 20%.

#### V. THE VSY FORMULA

The Van Regemorter formula (3) is most accurate for  $x \gg 1$ . Therefore, this formula fits applications which require accurate account of suprathermal electrons (e.g., pulsed power devices, subpicosecond lasers, solar flares). However, there are non-Maxwellian plasmas with overpopulated low-energy part of the electron distribution function, e.g., plasmas produced by UHF devices or by lasers with non-relativistic intensity of radiation (for our example, it is enough to have a free electron oscillation energy less than mean energy of the electron chaotic motion). Estimates of kinetic coefficients for such plasmas require cross sections accurate in low-energy range ( $x = 1 \div 10$ ). Semiempirical formula suitable for this case was suggested by Vainshtein, Sobel'man, and Yukov [11,2]. We rewrite it as follows

$$\sigma_{z,n,n'}^{VSY}(x) = \frac{\pi a_0^2}{\sqrt{n'}} \left( \frac{\mathcal{R}}{I_n - I_{n'}} \right)^2 \left( \frac{I_{n'}}{I_n} \right)^{3/2} \frac{F(x)}{x} \quad (5)$$

where  $I_n$  is the optical electron binding energy and

$$F(x) = 14.5 \ln x + 4.15 + 9.15x^{-1} + 11.9x^{-2} - 5.16x^{-3} \quad (6)$$

is the fitting function which provides good fit to CC, CCC, and CBE cross sections discussed above. Being interested in an easy-to-use formula, we looked for function  $F(x)$  independent on  $z$ ,  $n$ , and  $n'$  although initially [11,2] functions  $F(x)$  were fitted to each of the transition studied. Using the expression  $I_n = \mathcal{R}z^2n^{-2}$  for the binding energy, formula (5) may be presented as follows

$$\sigma_{z,n,n'}^{VSY}(x) = \frac{\pi a_0^2}{z^4} n^7 \sqrt{n'} [(n')^2 - n^2]^{-2} \frac{F(x)}{x}. \quad (7)$$

Function (6) is shown by bold solid curve in Fig. 12. Dotted curves demonstrate functions  $F_{nn'}(x)$  obtained by replacing  $\sigma_{z,n,n'}^{VSY}(x)$  in expression (7) by functions (2):

$$F_{nn'}(x) = \frac{z^4 x \sigma_{z,n,n'}^f(x) [(n')^2 - n^2]^2}{\pi a_0^2 n^7 \sqrt{n'}}.$$

These dotted curves are not labeled because they are shown only for demonstrating their small deviation from function  $F(x)$ . Bold dash curves show  $\pm 30\%$  corridor around  $F(x)$  while bold dot-dash curves show  $\pm 50\%$  corridor. One can see that for  $x < 2$  the VSY formula is accurate to within 30%. For  $x = 1 \div 10$  this formula is accurate to within 50%. For larger electron energy ( $x > 10$ ), estimates of the cross sections are more accurate if based on the Van Regemorter formula (3).

## VI. CONCLUSIONS

We have presented CCC and CBE cross sections for electron-impact-induced transitions  $n \rightarrow n'$  in hydrogen-like ions  $C^{5+}$ ,  $Ne^{9+}$ ,  $Al^{12+}$ , and  $Ar^{17+}$  ( $n < n' \leq 6$ ).

With coefficients given in Table 1, expression (2) fits all CC, CCC, and CBE cross sections available for  $z = 6 \div 26$  to better than 10%, except for transition  $5 \rightarrow 6$  in  $C^{5+}$  which deviates from total  $z^4$ -scaling by 17%.

In general, a scaling of the cross sections over  $z^4$  is accurate to within a few percent for ions with large nuclear charge ( $z \gg 1$ ) but for ions with  $z \sim 1$ , a deviation from the scaling is significant (at  $x \sim 1$ ). For  $x \gg 1$  the  $z^4$ -scaling is accurate for all ions and transitions. For each  $z$ , the accuracy of the scaling is higher for larger transition energy.

Semiempirical formulae (3) and (7) together provide an accuracy to within 50% for any energy: for  $x < 2$  the VSY formula (7) is accurate to within 30%; for  $2 < x < 10$  this formula is accurate to within 50%; for  $x > 10$  an accuracy to better than 50% is provided by the Van Regemorter formula (3).

## VII. ACKNOWLEDGMENTS

This work was supported by the Israel Academy of Science, The Ministry of Science and the Arts, and the Ministry of Absorption. In part (L.V.) the work was supported by Moscow International Science and Technology Center (grant 07-95) and Russian Basic Research Fond (grant 94-2-05371). Research of I. Bray is sponsored in part by the Phillips Laboratory, Air Force Materiel Command, USAF, under cooperative agreement number F29601-93-2-0001. The views and conclusions contained in this document are those of the authors and should not be interpreted as necessarily the official policies or endorsements, either expressed or implied, of Phillips Laboratory or the U.S. Government.

- 
- [1] V. P. Shevelko and L. A. Vainshtein, *Atomic Physics for Hot Plasmas* (IPP, Bristol, 1993).
  - [2] I. I. Sobel'man, L. A. Vainshtein, and E. A. Yukov, *Excitation of Atoms and Broadening of Spectral Lines*, (Springer, 1995).
  - [3] I. Bray, Phys. Rev. A **49**, 1066 (1994).
  - [4] I. Bray and A. T. Stelbovics, in *Advances in Atomic, Molecular, and Optical Physics*, Vol 35 edited by B. Bederson and H. Walther (Academic Press, San Diego, 1995)
  - [5] I. Bray, I. E. McCarthy, J. Wigley, and A. T. Stelbovics, J. Phys. B **23**, L831 (1993); B **29**, L245 (1996).
  - [6] S. A. Wakid and J. Callaway, Phys. Letters **81** A, 333 (1981).
  - [7] N. Abu-Salbi and J. Callaway, Phys. Rev. A **24**, 2372 (1981).
  - [8] D. H. Oza, J. Callaway, and N. Abu-Salbi, Phys. Rev. A **25**, 2812 (1982).
  - [9] A. K. Pradhan and J. W. Gallagher, At. Data Nucl. Data Tables, **52**, 227 (1992).
  - [10] J. Callaway, At. Data Nucl. Data Tables, **57**, 9 (1994).
  - [11] L. A. Vainshtein, I. I. Sobel'man, and E. A. Yukov, *Electron-Impact Excitation Cross Sections for Atoms and Ions*, (Nauka, Moscow, 1973), in Russian.
  - [12] C. P. Bhalla, S. R. Grabbe, and A. K. Bhatia, Phys. Rev. A **52**, 2109 (1995).
  - [13] R. Kisielius, K. A. Berrington, and P. H. Norrington, J. Phys. B **28**, 2459 (1995).
  - [14] L. A. Vainshtein (unpublished).
  - [15] Y.-K. Kim and J.-P. Desclaux, Phys. Rev. A **38**, 1805 (1988).
  - [16] H. Van Regemorter, Astrophys. J. **136**, 906 (1962).
  - [17] R. Mewe, Astron. Astrophys. **20**, 215 (1972).
  - [18] S. M. Younger and W. L. Wieze, J. Quant. Spectrosc. Radiat. Transfer **22**, 161 (1979).
  - [19] D. H. Crandall, in *Physics of Ion-ion and Electron-ion Collisions*, edited by F. Brouillard and J. W. McGowan (Plenum Press, New York, 1983), Chap. 4.

### VIII. FIGURE CAPTIONS

- Figure 1a.** Scaled cross sections for transition  $1 \rightarrow 2$  in hydrogen-like ions with  $z = 6 \div 26$ .  
**Figure 1b.** Fragment of Figure 1a.  
**Figure 2.** Scaled cross sections for transition  $1 \rightarrow 3$  in hydrogen-like ions with  $z = 6 \div 18$ .  
**Figure 3.** Scaled cross sections for transition  $1 \rightarrow 4$  in hydrogen-like ions with  $z = 6 \div 18$ .  
**Figure 4.** Scaled cross sections for transition  $2 \rightarrow 3$  in hydrogen-like ions with  $z = 6 \div 18$ .  
**Figure 5.** Scaled cross sections for transition  $2 \rightarrow 4$  in hydrogen-like ions with  $z = 6 \div 18$ .  
**Figure 6.** Scaled cross sections for transition  $3 \rightarrow 4$  in hydrogen-like ions with  $z = 6 \div 18$ .  
**Figure 7.** Scaled CBE cross sections for transitions  $n \rightarrow 5$  in hydrogen-like ions with  $z = 6 \div 18$ .  
**Figure 8.** Scaled CBE cross sections for transitions  $n \rightarrow 6$  in hydrogen-like ions with  $z = 6 \div 18$ .  
**Figure 9.** Scaled CC, CCC, and CBE cross sections for transition  $1s \rightarrow 2s$  in hydrogen-like ions with  $z = 6 \div 26$ .  
**Figure 10.** Scaled CC, CCC, and CBE cross sections for transition  $1s \rightarrow 2p$  in hydrogen-like ions with  $z = 6 \div 26$ .  
**Figure 11.** Gaunt factor  $G(x)$  for the Van Regemorter formula (3). Dotted curves demonstrate functions  $G_{nn'}(x)$ .  
**Figure 12.** Function  $F(x)$  for the VSY formula (7). Dotted curves demonstrate functions  $F_{nn'}(x)$ .

### IX. TABLE 1

| $n$ | $n'$ | $\alpha_{nn'}$ | $\beta_{nn'}$ | $\gamma_{nn'}$ | $\delta_{nn'}$ | $\zeta_{nn'}$ |
|-----|------|----------------|---------------|----------------|----------------|---------------|
| 1   | 2    | 3.22           | 0.357         | 0.00157        | 1.59           | 0.764         |
| 1   | 3    | 0.452          | 0.723         | 0.0291         | -0.380         | 0.834         |
| 1   | 4    | 0.128          | -0.0300       | 0.163          | -0.150         | 0.185         |
| 1   | 5    | 0.0588         | -0.0195       | 0.0803         | -0.0649        | 0.0776        |
| 1   | 6    | 0.0321         | -0.0115       | 0.0458         | -0.0374        | 0.0441        |
| 2   | 3    | 173            | 46.7          | -94.5          | 358            | -102          |
| 2   | 4    | 16.7           | -8.32         | 12.6           | 22.5           | -3.44         |
| 2   | 5    | 4.47           | -5.54         | 8.10           | 3.52           | 0.820         |
| 2   | 6    | 1.94           | -2.69         | 4.43           | 0.461          | 1.54          |
| 3   | 4    | 1880           | 204           | -1280          | 4860           | -1620         |
| 3   | 5    | 164            | -236          | 128            | 458            | -247          |
| 3   | 6    | -2.71          | -468          | 268            | 161            | -304          |
| 4   | 5    | 4800           | -55100        | 18100          | 41400          | -48800        |
| 4   | 6    | 456            | -4530         | 2230           | 2870           | -3570         |
| 5   | 6    | 75000          | 247000        | -172000        | 84700          | 123000        |

**Table 1.** Coefficients  $\alpha_{nn'}$ ,  $\beta_{nn'}$ ,  $\gamma_{nn'}$ ,  $\delta_{nn'}$ , and  $\zeta_{nn'}$  for fitting function (2).

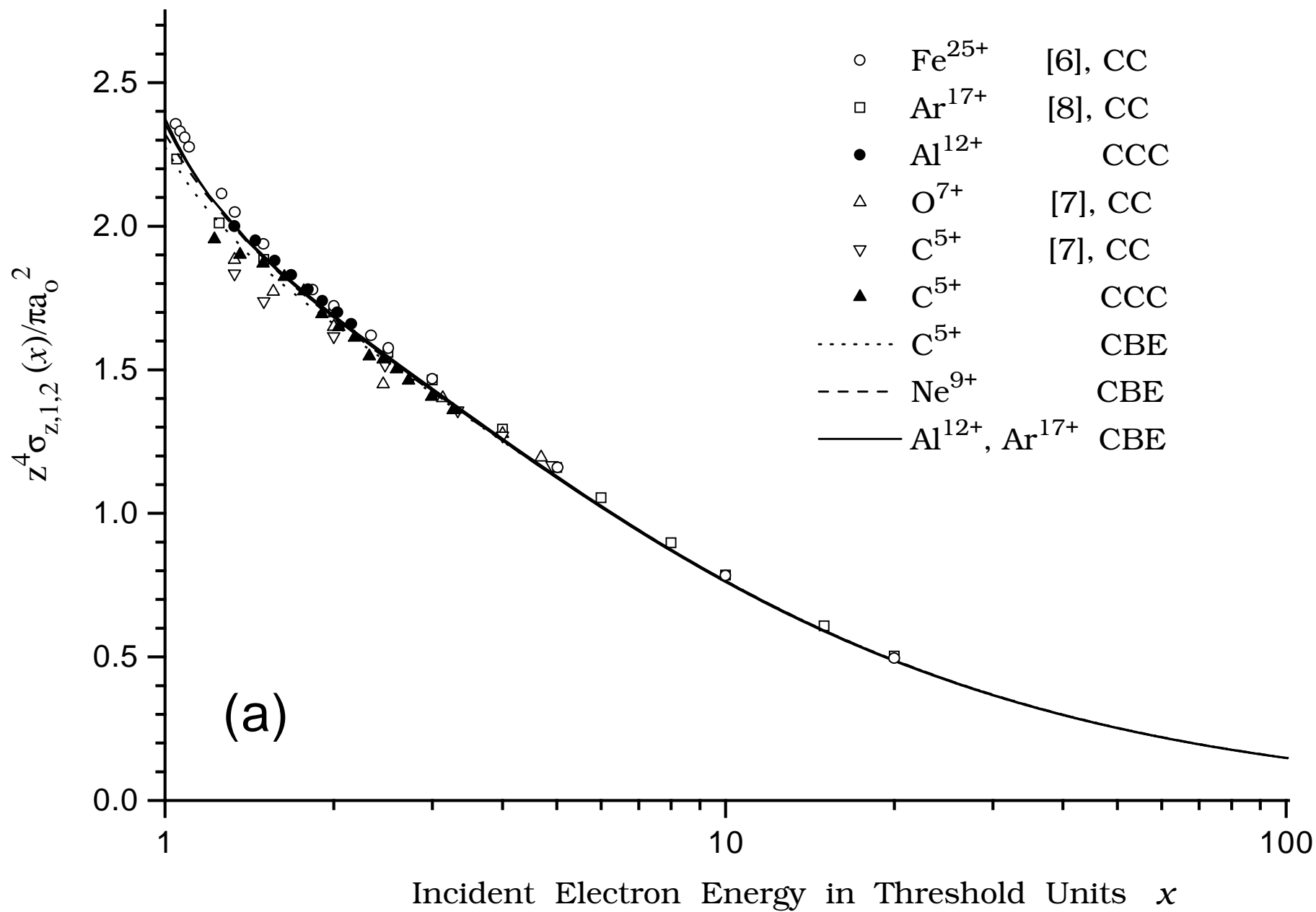


figure 1(a)

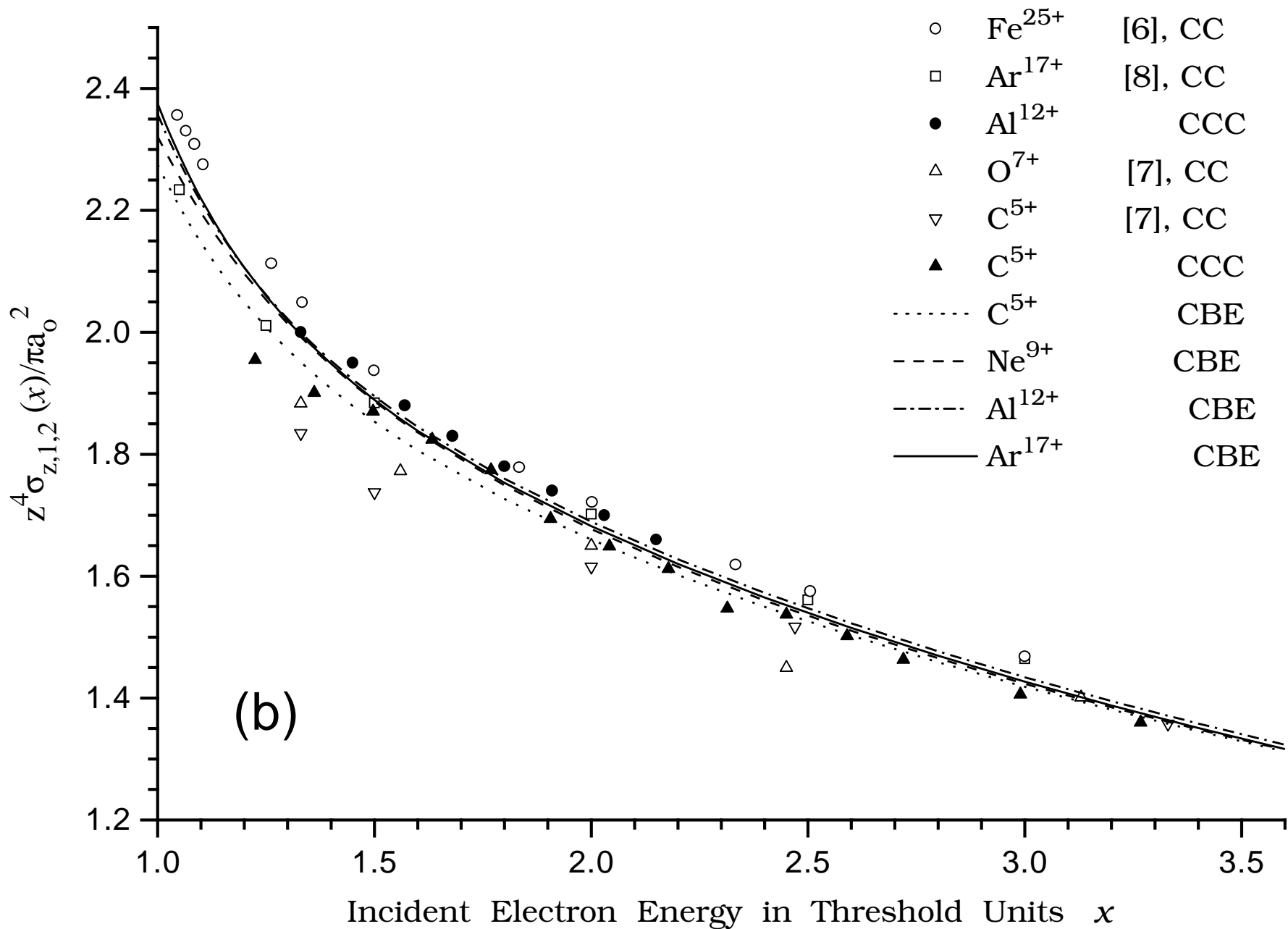
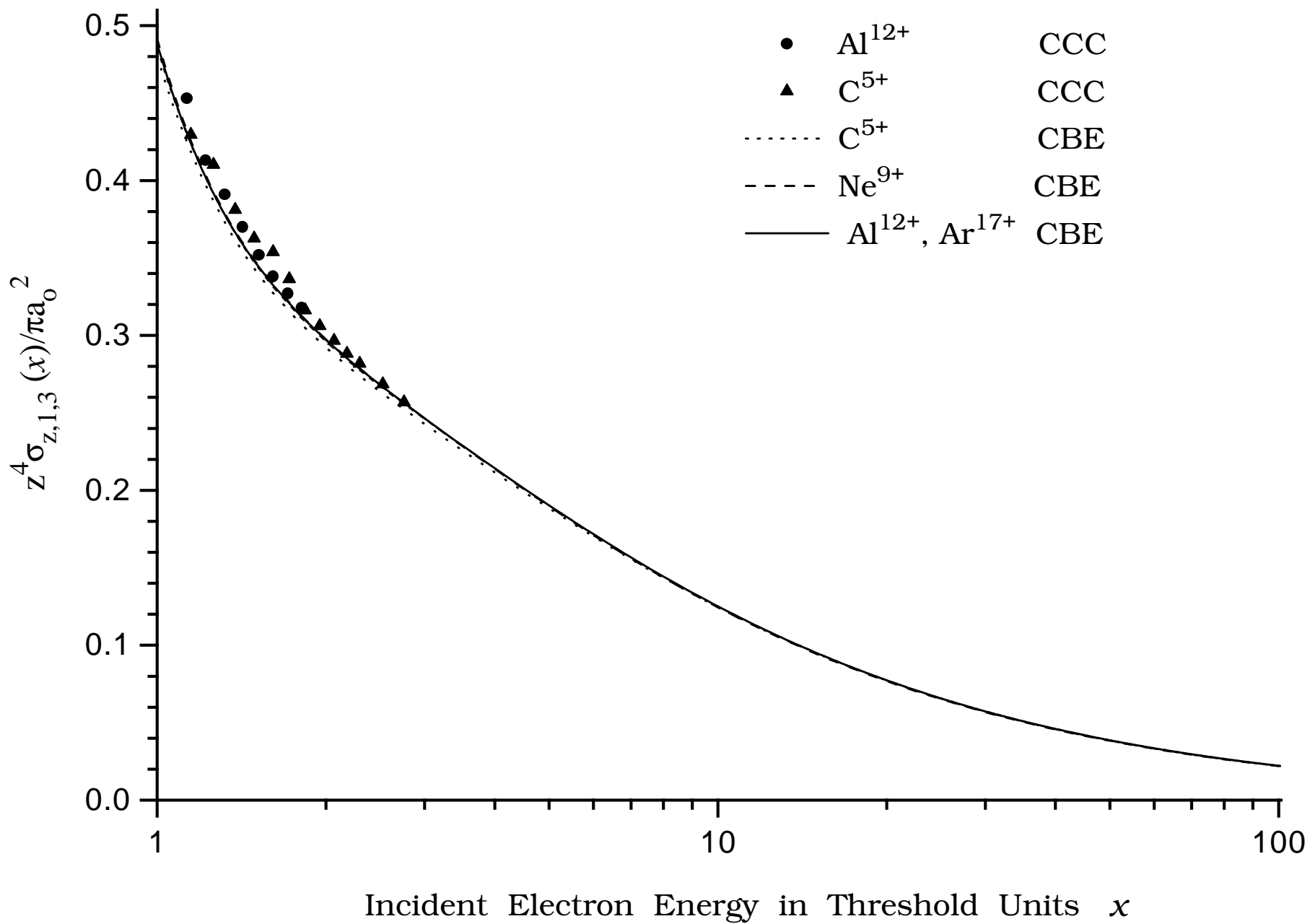
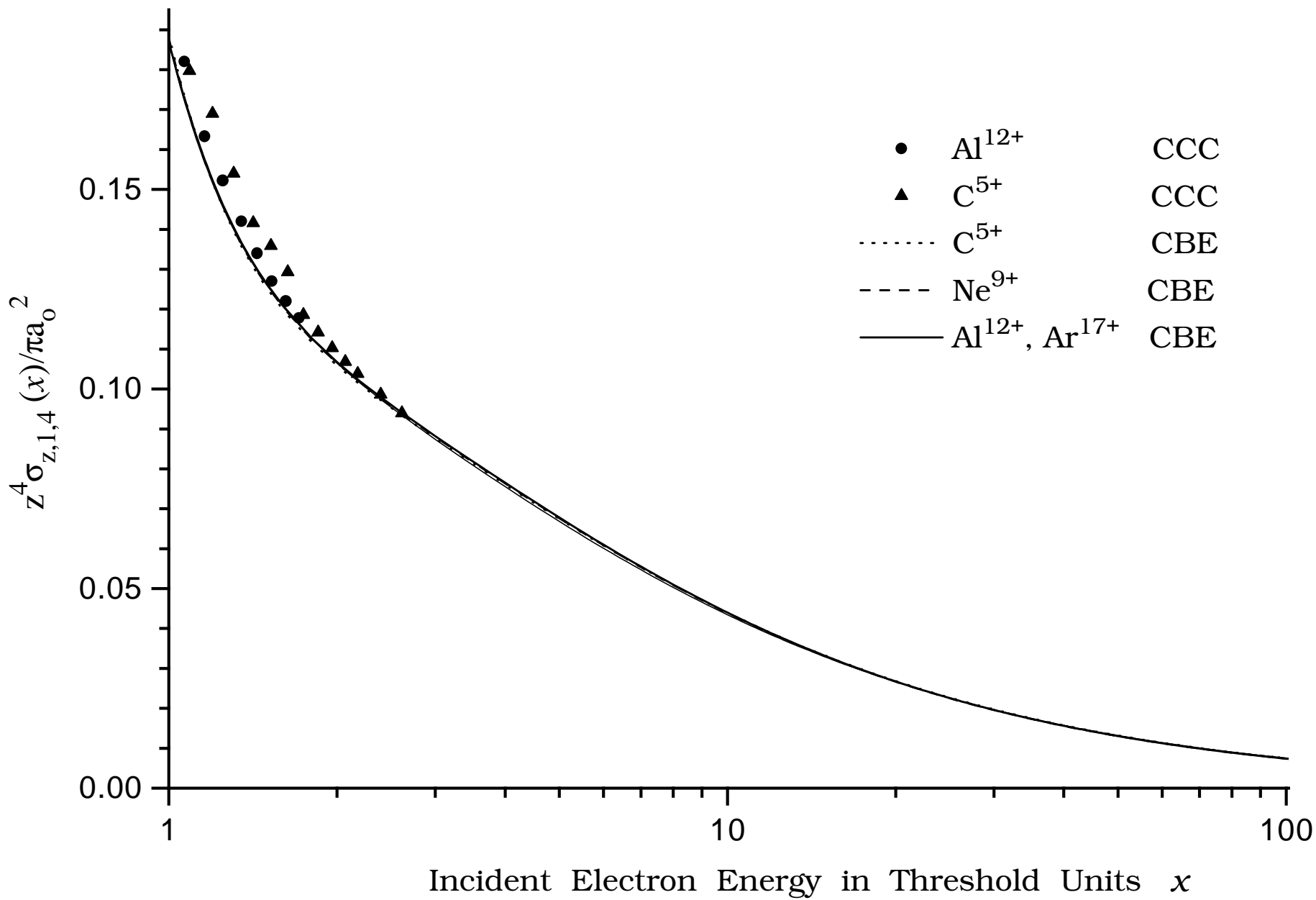


figure 1(b)



**figure 2**



**figure 3**

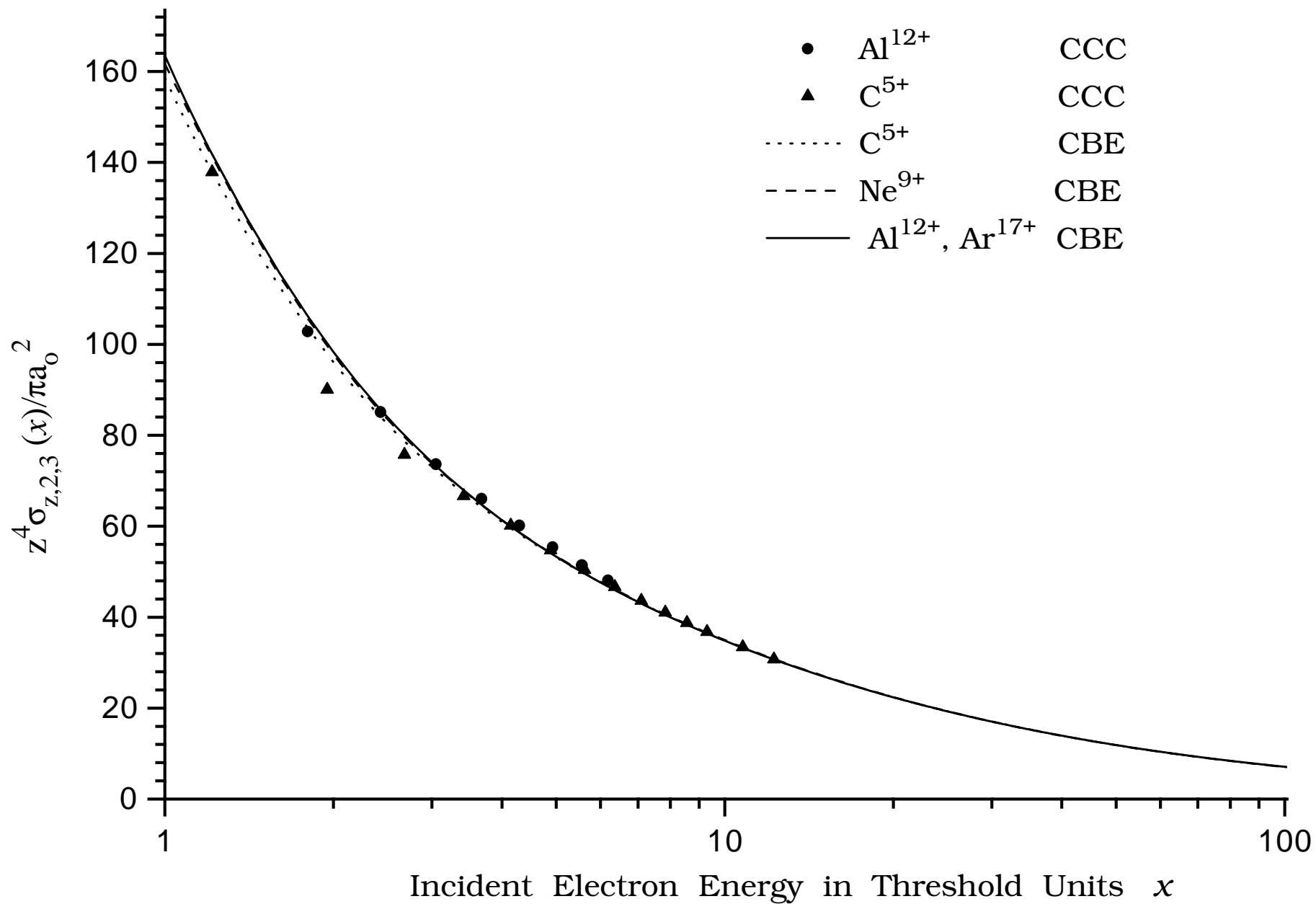


figure 4

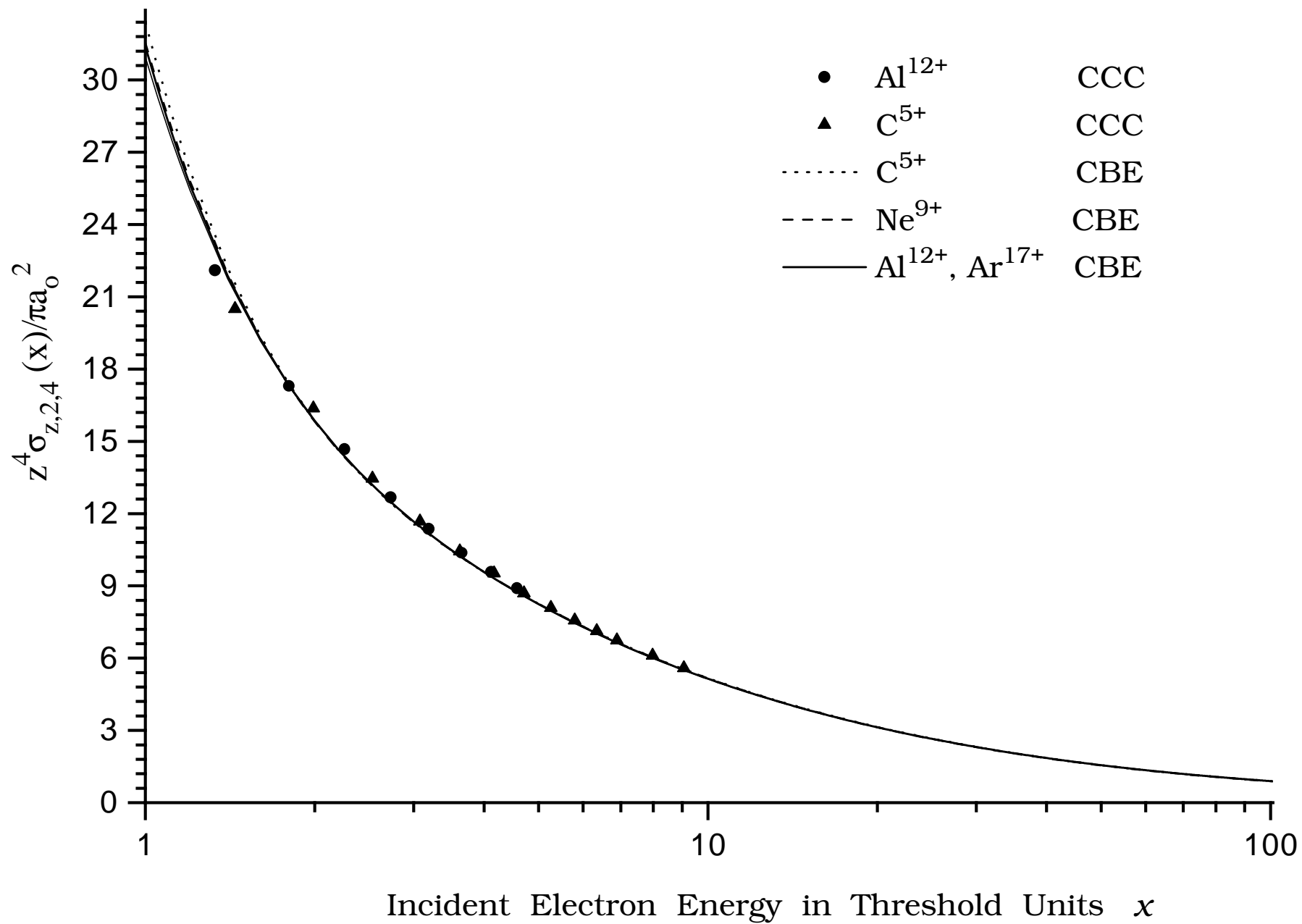


figure 5

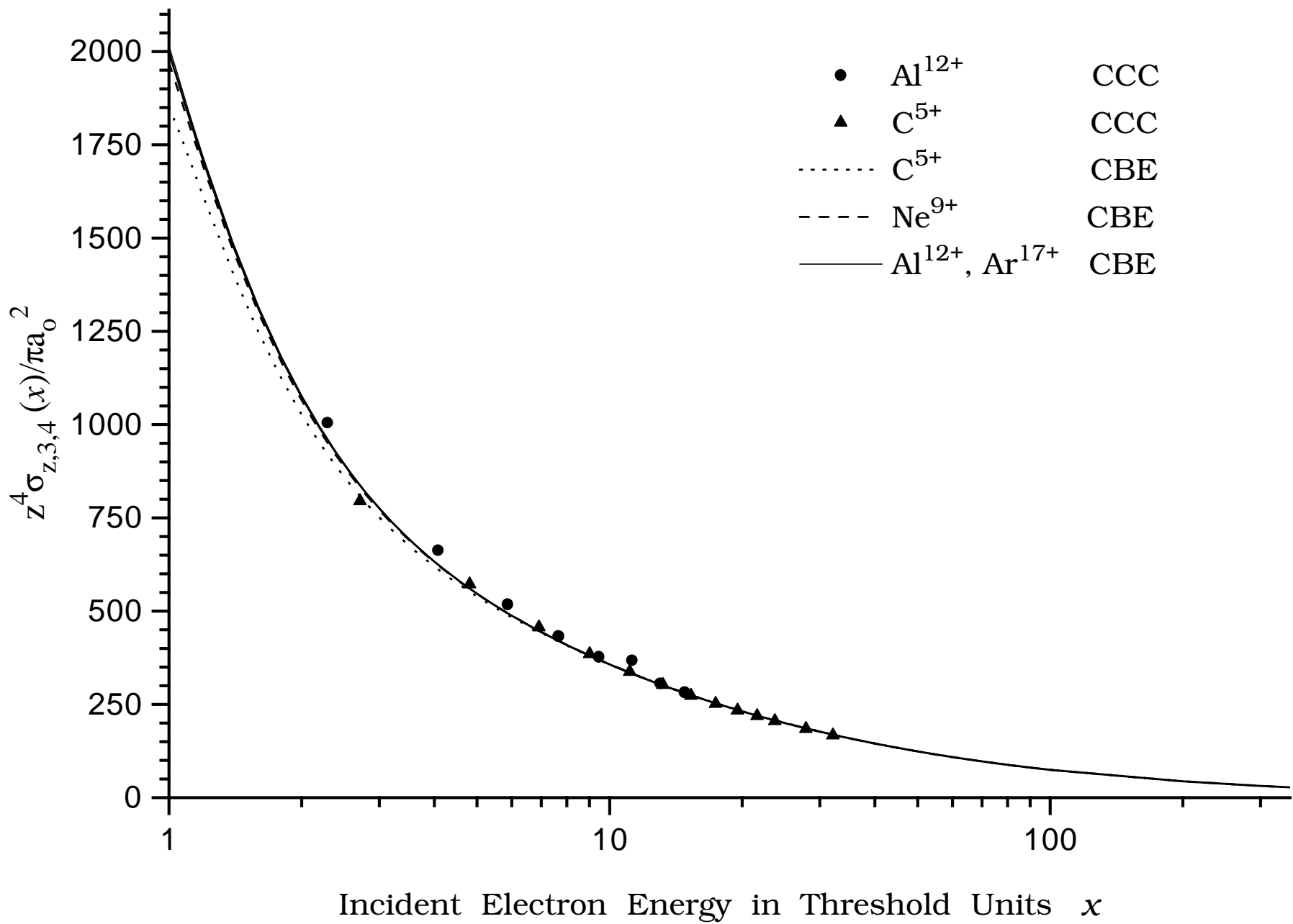
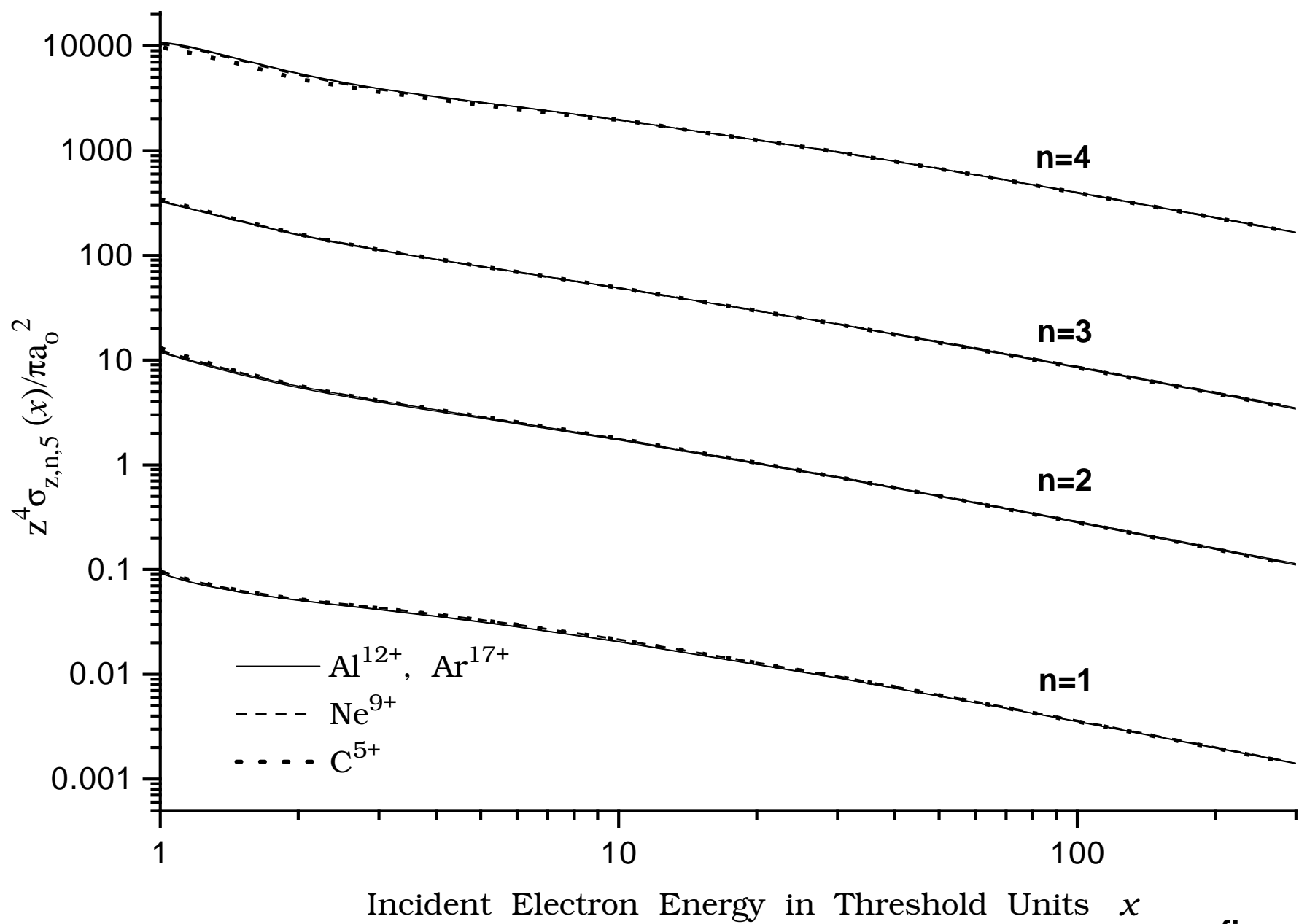
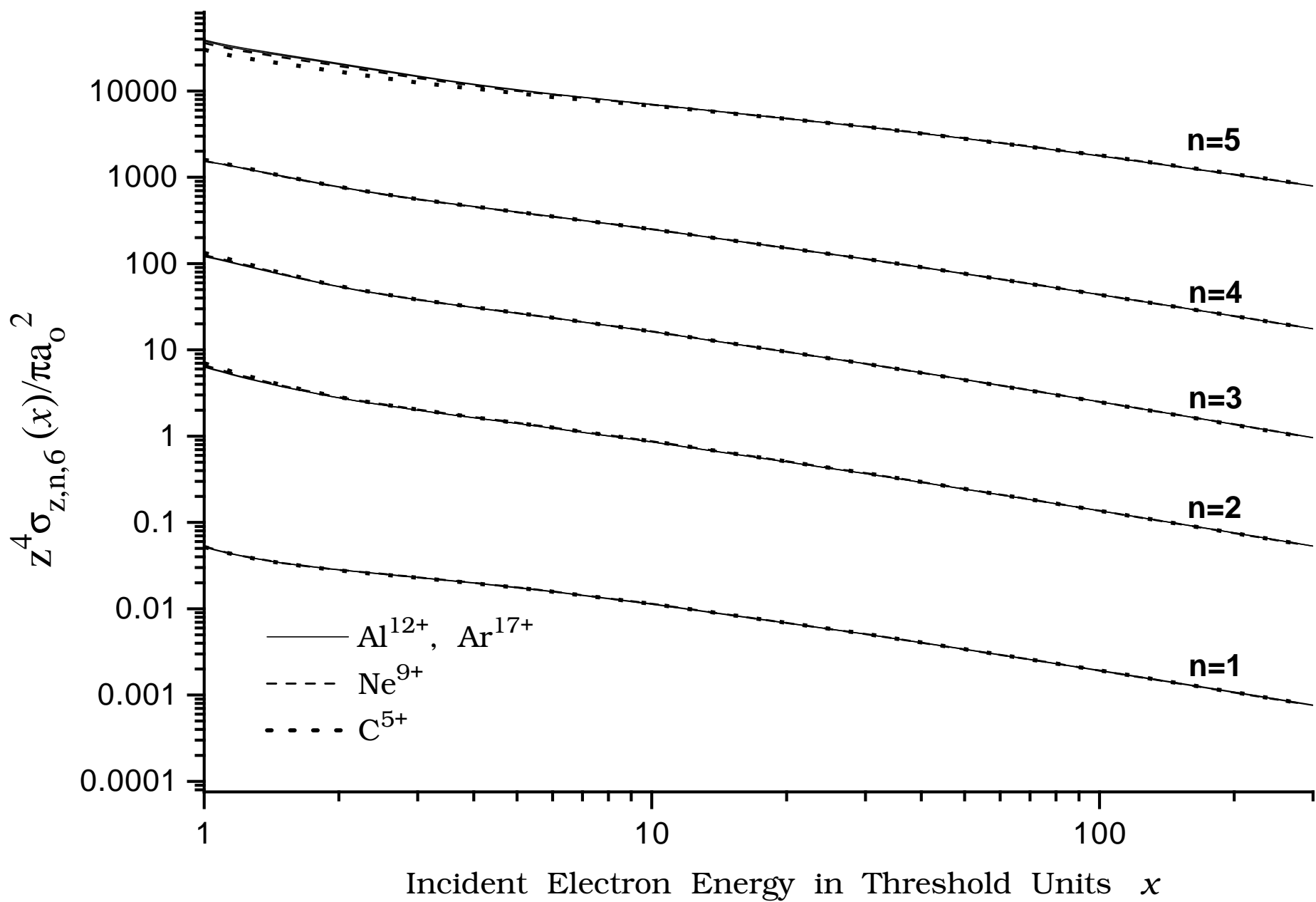


figure 6



**figure 7**



**figure 8**

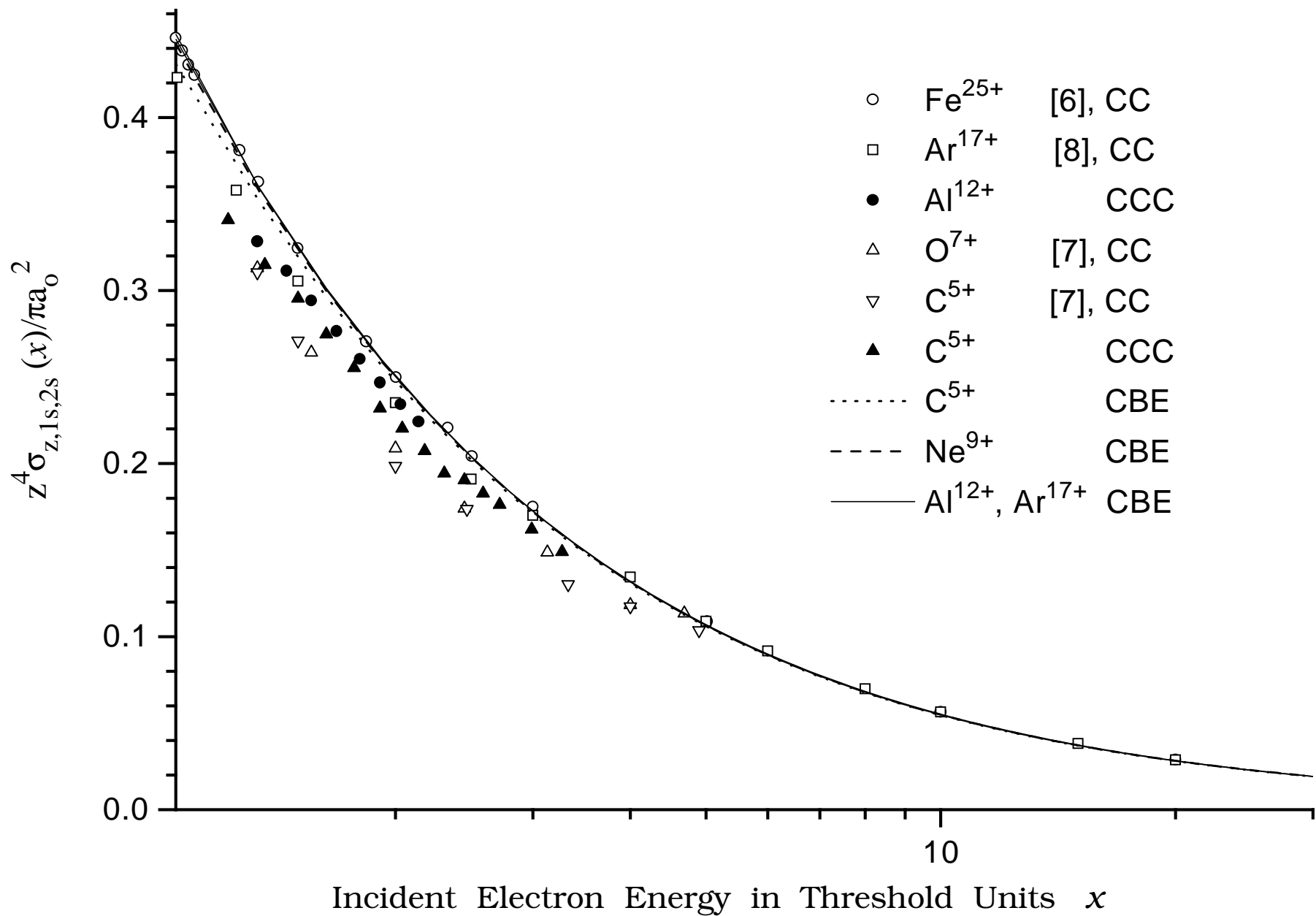


figure 9

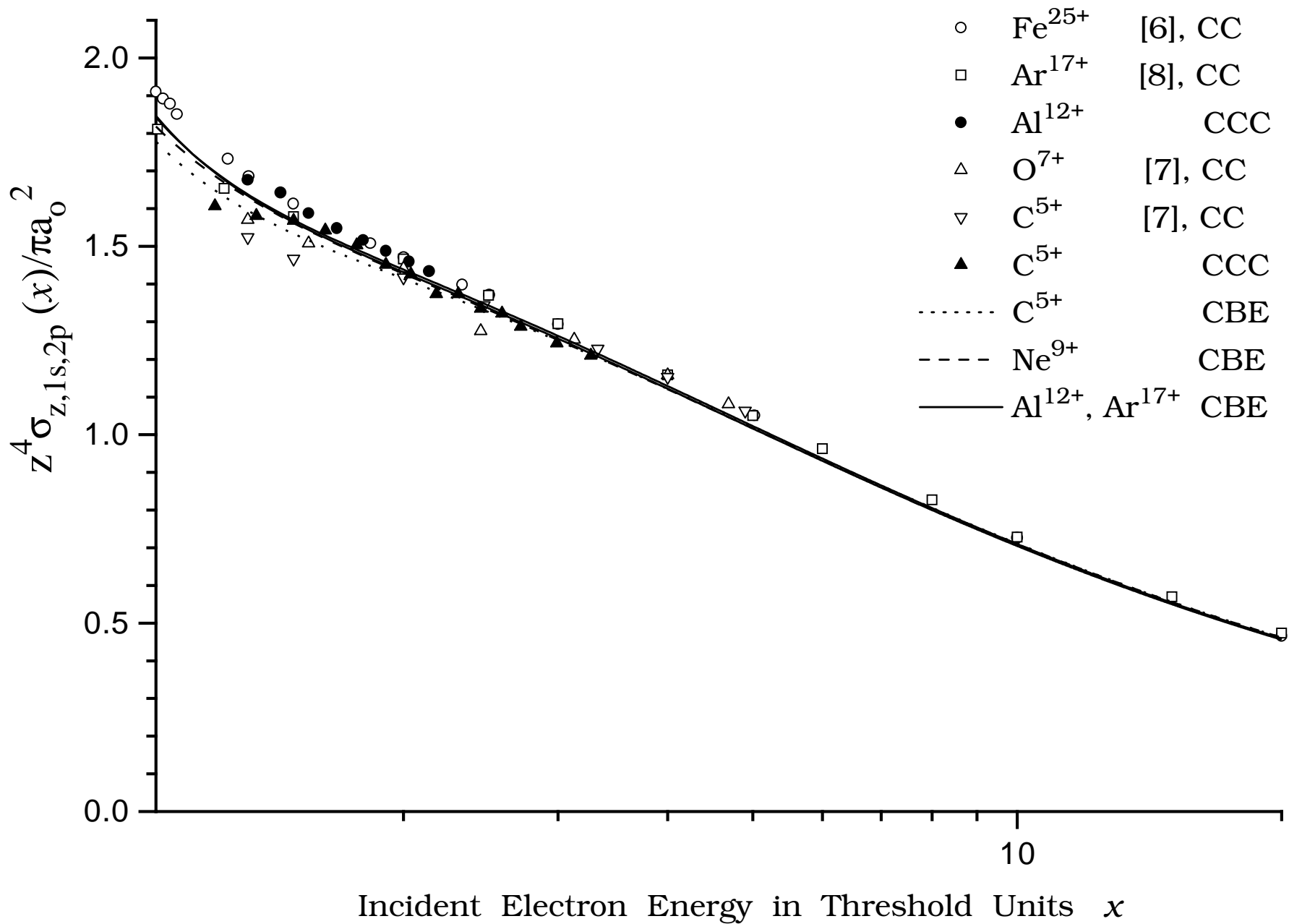


figure 10

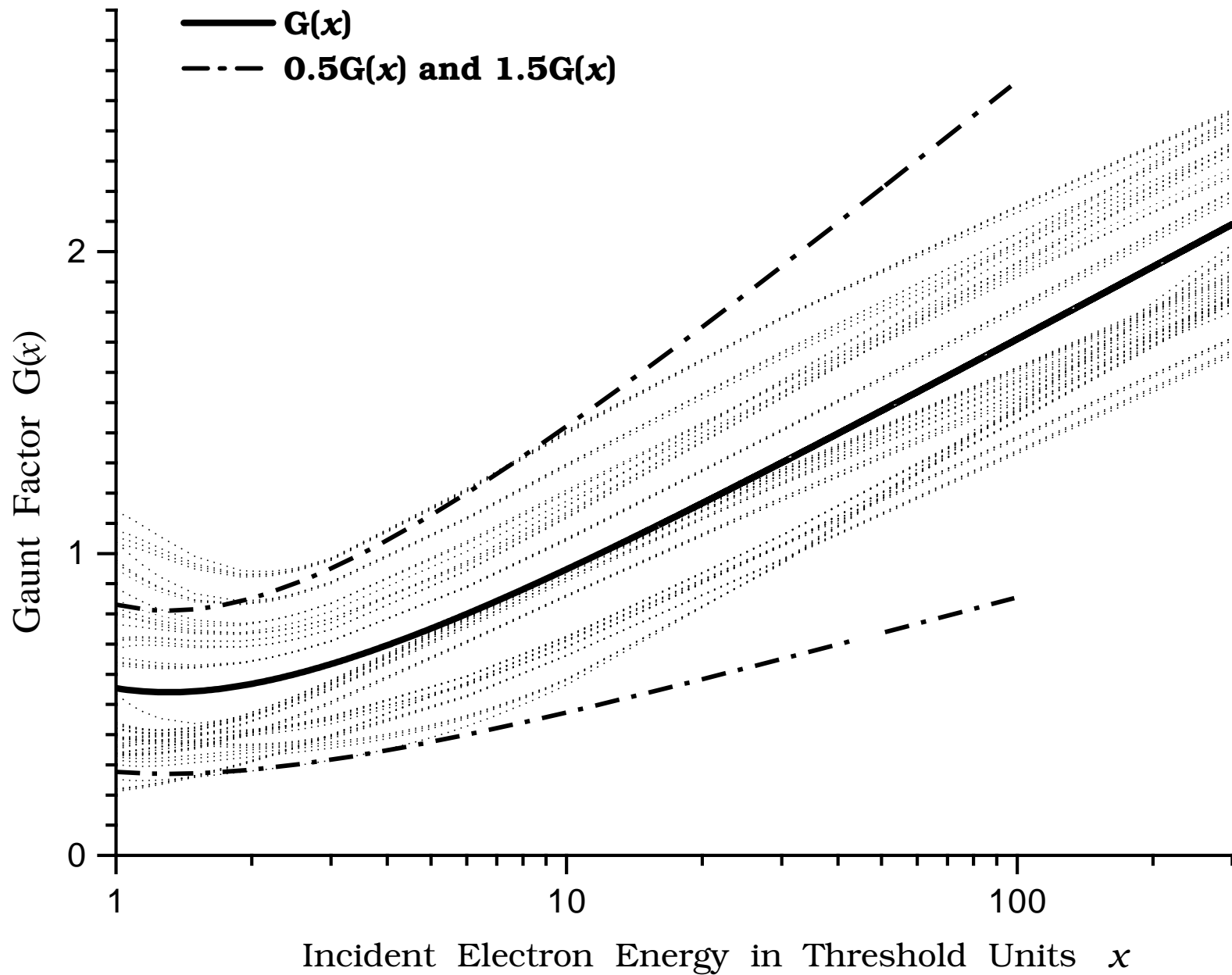


figure 11

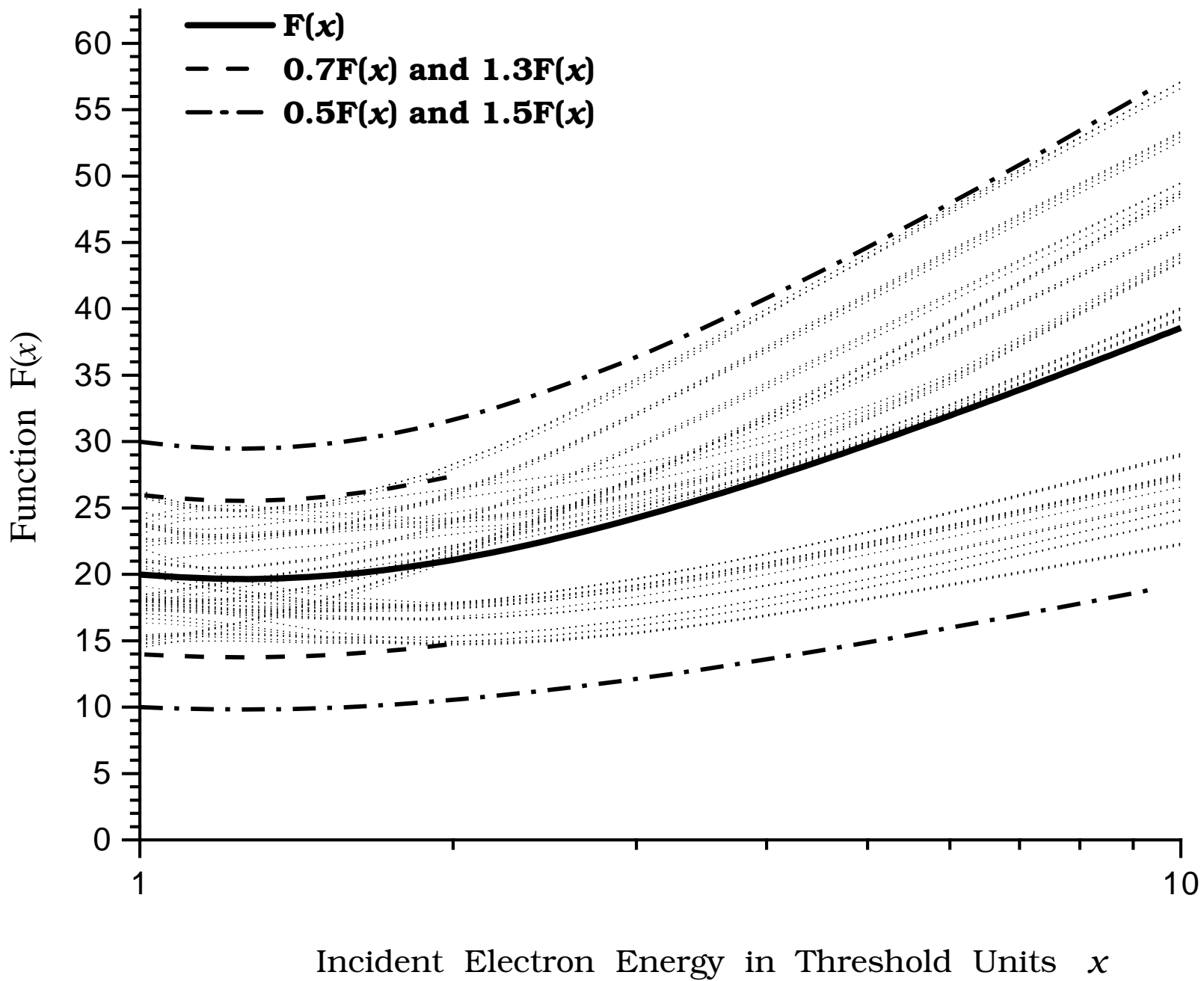


figure 12